Supplementary Information for
The Dynamics and Energy Landscape of DNA Plectoneme Nucleation

Philipp U. Walker[1], *Willem Vanderlinden*[1,2], *Jan Lipfert*[1,*]

[1]Department of Physics, Nanosystems Initiative Munich, and Center for Nanoscience, LMU Munich, Amalienstrasse 54, 80799 Munich, Germany
[2]Department of Chemistry, KU Leuven, Celestijnenlaan 200F, 3001 Heverlee, Belgium
[*]Correspondence : Email: Jan.Lipfert@lmu.de; Phone: +49-8921802005

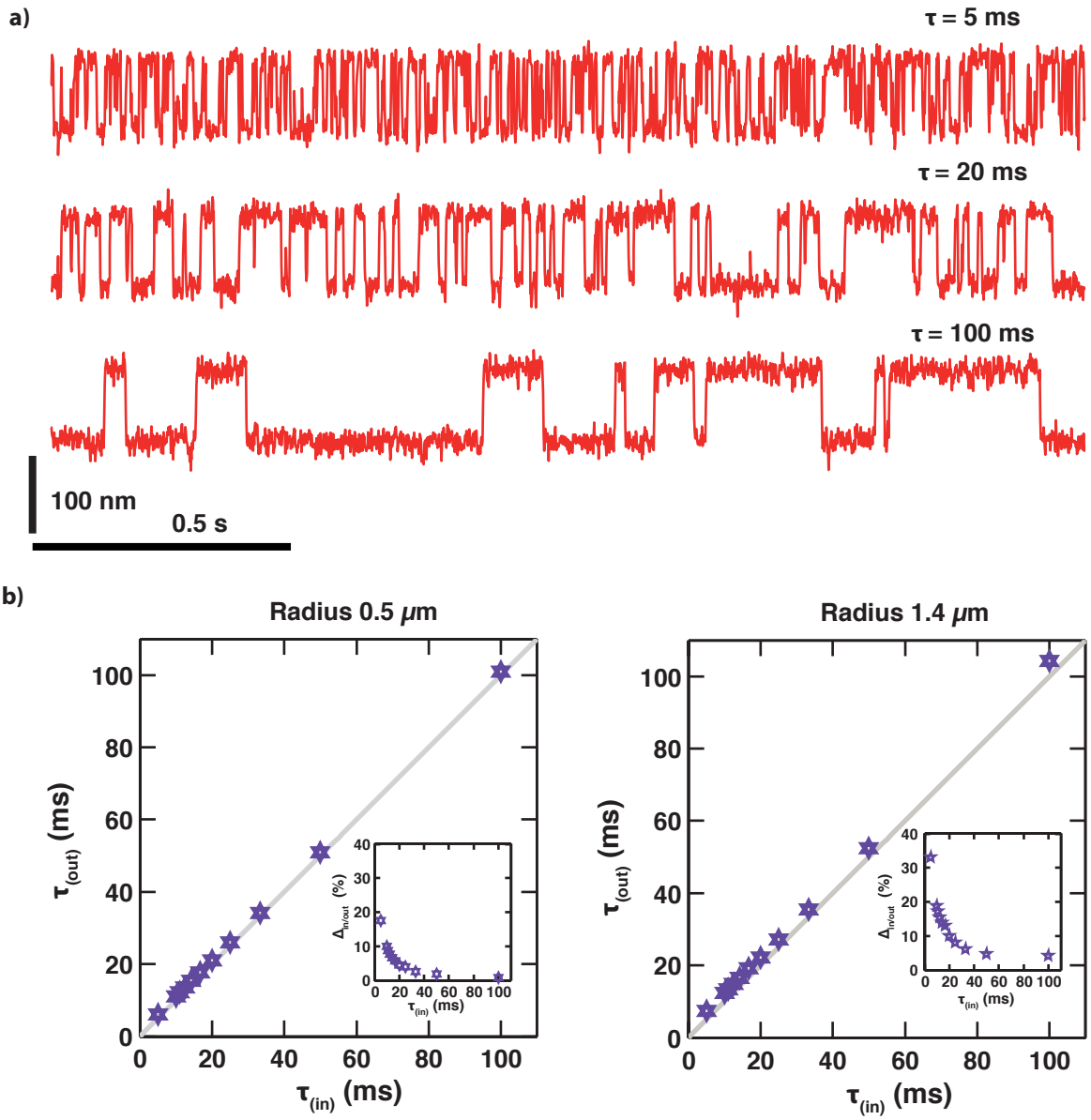

Figure S1. Testing the time resolution limits using Brownian dynamics simulations of the bead-DNA system. a) Simulated extension traces for different hopping rates (mean dwell time from 5 to 100 ms) at buckling equilibrium. Traces are obtained by numerically simulating the Langevin equation of the bead subject to external forces from the magnets and the DNA tether (see "***Simulations of the DNA-bead system in the MT***"). Instantaneous 100 nm jumps in the extension were added randomly with exponentially distributed dwell times and a predefined rate. (b) Mean dwell time used as input parameter in the simulation τ_{in} vs. mean dwell time determined by the analysis of the final simulated traces τ_{out} for two different bead sizes used in the measurements. Gray line is the line $\tau_{in} = \tau_{out}$. The insets give the relative error of τ_{out} compared to the known τ_{in}. Time steps for the simulation were set to 0.01 ms, the camera frequency to 1 kHz. The analysis of the simulated extension traces was performed using the same filters and analysis routines as used in the analysis of the measured traces.

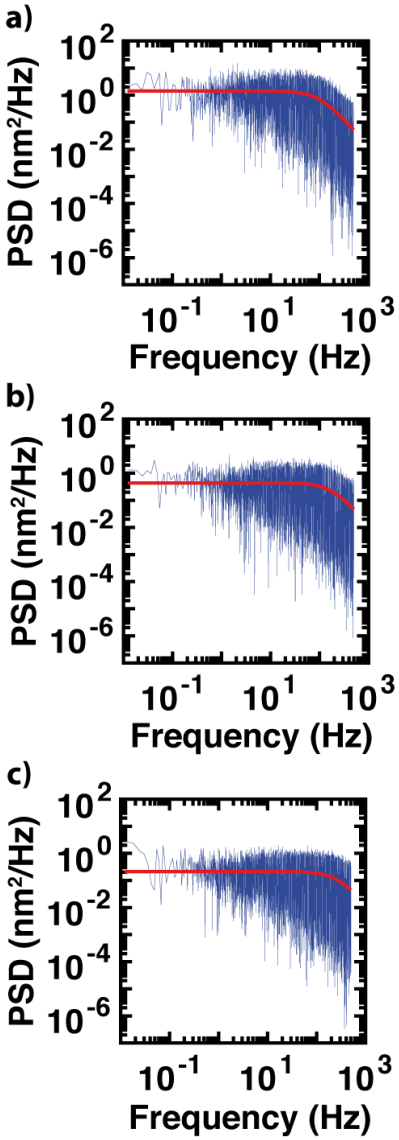

Figure S2. Power spectral density of extension fluctuations for DNA-tethered beads. The PSD of a torsional unconstrained DNA molecule at 100 mM NaCl at a) 2pN, b) 3 pN, c) 4pN. The corner frequencies differ with force, but not with salt and lead to a mean value of 98 ± 3 Hz, 161 ± 6 Hz and 230 ± 12 Hz for 2, 3 and 4 pN (means and standard errors from 4 independent measurements at each force), respectively. Red lines are Lorentzian fits to the data.

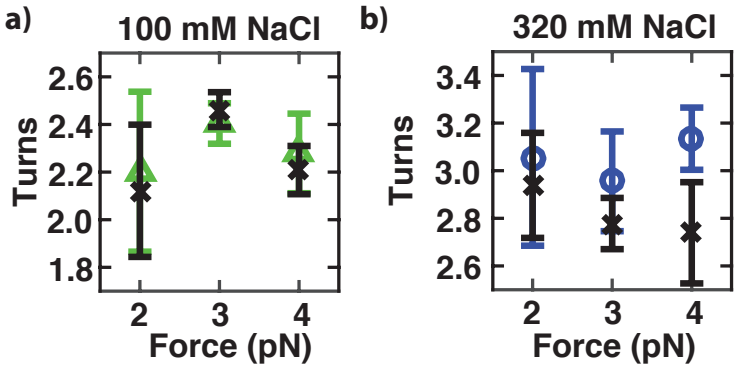

Figure S3. Comparison of the sum of ΔWr_{pre} and ΔWr_{post} to direct measurements of ΔWr_b. For 100 mM NaCl (a) as well as 320 mM NaCl (b) the absolute values of ΔWr_{pre} and ΔWr_{post} add up to ΔWr_b to within experimental error (color code according to Fig. 2, black crosses are the sum of ΔWr_{pre} and ΔWr_{post}).

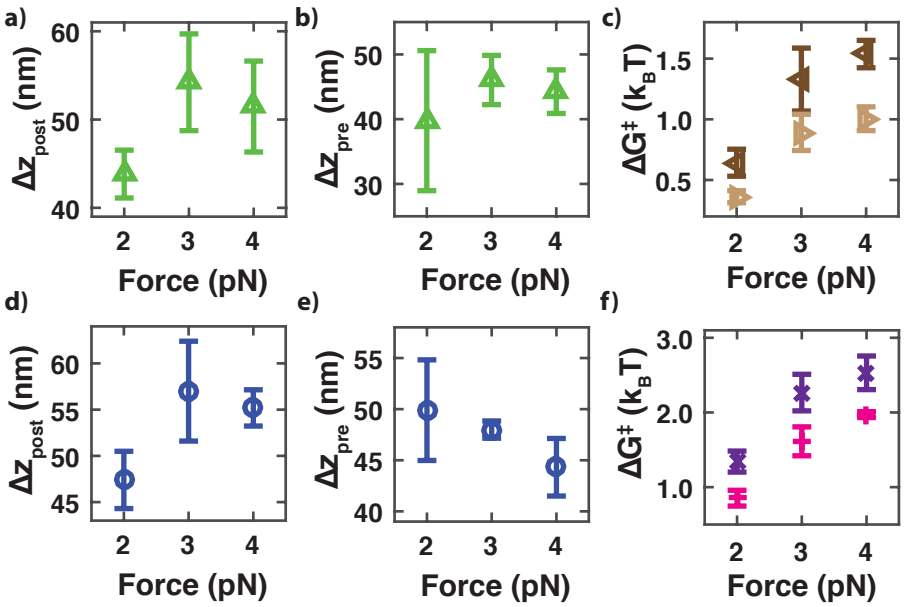

Figure S4. Additional analyses of the buckling energy landscape. a) and d) Distances of the maximum of the energy barrier to the post-buckling minimum along the extension axis determined from the reconstructed energy landscapes for 100 mM NaCl (a) and for 320 mM NaCl (d). No force dependency of the distances between the maxima and the minima is observed. b) and e) Distances of the maximum of the energy barrier to the pre-buckling minimum along the extension axis determined from the reconstructed energy landscape. The distances to the transition state obtained by the energy landscape indicate no significant force dependency for 100 mM NaCl (b) or for 320 mM NaCl (e). (c) and (f) Height of the energy barriers at $P_{post} = 0.5$ from the post-buckling state and from the pre-buckling state. The energy barrier $\Delta G^{\#}_{pre}$ was determined from the minimum of the pre-buckling state to the maximum of the energy barrier (dark brown left-pointing triangle: 100 mM NaCl, purple cross: 320 mM). Analogously, $\Delta G^{\#}_{post}$ from the minimum of the post-buckling state to the maximum of the energy barrier was obtained (brown right-pointing triangle: 100 mM NaCl, pink plus: 320 mM NaCl). For both salt conditions and at every force measured, $\Delta G^{\#}_{post}$ is smaller than $\Delta G^{\#}_{pre}$.

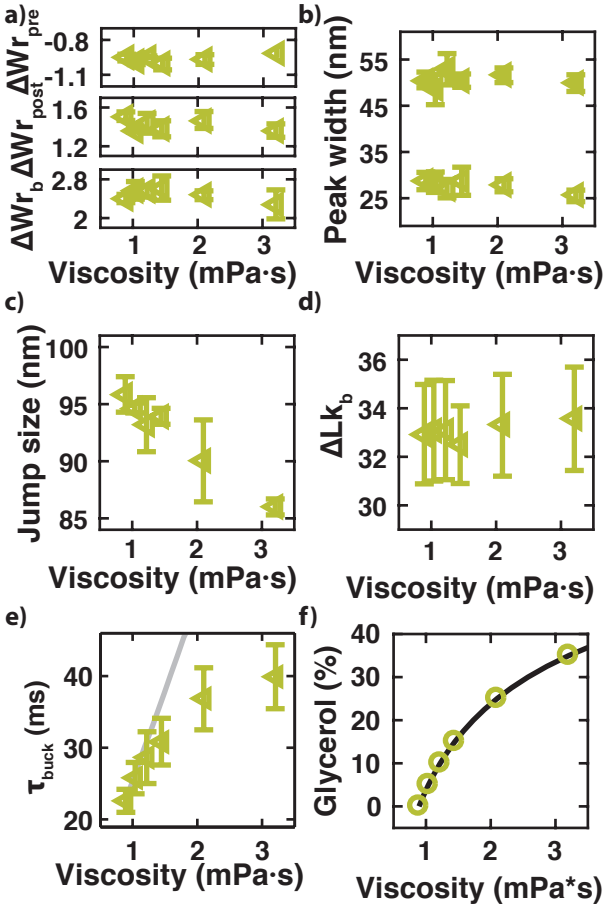

Figure S5. Effect of glycerol on buckling dynamics and equilibrium properties. All data were recorded at constant force and salt (3 pN, 100 mM NaCl). (a) Effect of friction on distance to transition state in turns. Addition of glycerol does not change the distance to the transition state in number of turns, neither for the pre- nor post-buckling state. Furthermore the number of turns converted from twist to writhe does not change by friction. (b) Peak width of pre- and post-buckling state vs. friction. The peak widths of all measured frictions remain constant and show no influence by glycerol. (c) Jump size at the buckling point vs. friction. A slight trend of reduction in the jump size with higher glycerol concentration and therefore higher friction is observed. Nevertheless we note that most of the data points lie within the error bars. (d) Buckling point ΔLk_b vs. friction. An increase in glycerol concentration and thus in friction does not change ΔLk_b. For every measurement point in all panels three different DNA-bead combinations were measured. Before analyzing, all extension traces were corrected for the change in the index of refraction due to glycerol. (e) Influence of friction on the characteristic buckling time. An increase in friction by glycerol leads to a longer characteristic dwell time. A simple linear fit does not describe the behavior. Gray line extrapolated according to Bai et. al with measurement value without glycerol as starting point [1] (f) Relationship between viscosity and glycerol concentration. Data were taken from Ref. [2].

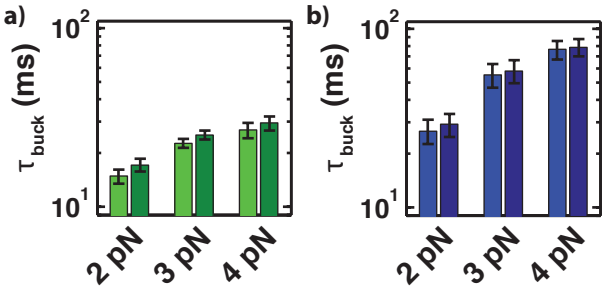

Figure S6. Effect of the correction of the buckling times for finite acquisition time. All buckling times reported in the manuscript, unless indicated otherwise, were corrected for the effect of finite acquisition time (see "***Correction for finite acquisition times***" section above). Biases due to the finite camera frequency are corrected by applying a correction based on the moment equations for a two-state Markov model. All corrected τ_{buck} are faster than the uncorrected τ^*_{buck}, but within the experimental error. a) Buckling times for DNA in 100 mM NaCl; light green: corrected values; dark green: uncorrected values. b) Buckling times for DNA in 320 mM NaCl; light blue: corrected values; dark blue: uncorrected values.

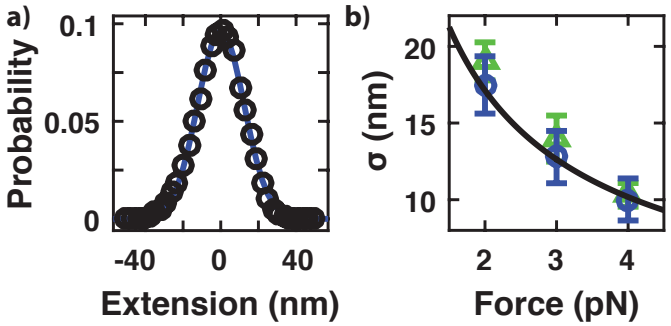

Figure S7. Magnitude of the extension fluctuations and estimate of the instrument response function S(z). (a) Histogram of extension fluctuations (black circles) and Gaussian fit (blue line), at 2 pN and 320 mM NaCl. The histogram of tether extension measurements for a torsional relaxed DNA tether is well described by a single Gaussian fit. Therefore the point spread function or instrument response S(z) used in the deconvolution procedure was set to a Gaussian distribution with peak width determined for every salt and force separately. (b) Standard deviation of extension fluctuations (σ_Z) vs. applied force for 100 mM (green triangle) and 320 mM (blue circle) NaCl. The magnitude of the extension fluctuations in the magnetic tweezers can be modeled by considering the Taylor expansion around the equilibrium position of the DNA-tethered bead and equipartition [3], yielding $\sigma_Z = (k_B T / \partial F/\partial L)^{1/2}$; $\partial F/\partial L$ is the derivative of force response of the tether with respect to the tether extension L. We approximate $\partial F/\partial L$ with the analytical derivative of the approximation formula by Bouchiat *et al*. [4] to the worm-like chain (WLC) model. The WLC model has two parameters: for the contour length, we use the value expected from the crystallographic length, 2700 nm for our 7.9 kbp DNA constructs; for the bending persistence length we use 45 nm, an average value determined previously for DNA under the salt conditions considered in our measurements. The prediction for σ_Z of the WLC model (black solid line) provides an excellent description of our data (reduced $\chi^2 = 1.08$ and 0.02 for 100 and 320 mM NaCl, respectively).

Supplementary References

[1] H. Bai, J. E. Kath, F. M. Zorgiebel, M. Sun, P. Ghosh, G. F. Hatfull, N. D. Grindley, and J. F. Marko, Proc Natl Acad Sci U S A **109**, 16546 (2012).
[2] N.-S. Cheng, Ind. Eng. Chem. Res. **47**, 3285 (2008).
[3] L. J. Vilfan I.D., Koster D.A., Lemay S.G., Dekker N.H. Magnetic tweezers for single-molecule experiments. In: Hinterdorfer P, van Oijen A, editors., Springer (2009).
[4] C. Bouchiat, M. D. Wang, J. Allemand, T. Strick, S. M. Block, and V. Croquette, Biophys J **76**, 409 (1999).